



Chemistry A European Journal

 **Chemistry
Europe**
European Chemical
Societies Publishing

Accepted Article

Title: Photophysical Properties and Heterogeneous Photoredox
Catalytic Activities of Ru(bpy)₃@InBTB MOF

Authors: In-Hwan Choi, Sukbin Yoon, SEONG HUH, Sung-Jin Kim,
and Youngmee Kim

This manuscript has been accepted after peer review and appears as an Accepted Article online prior to editing, proofing, and formal publication of the final Version of Record (VoR). This work is currently citable by using the Digital Object Identifier (DOI) given below. The VoR will be published online in Early View as soon as possible and may be different to this Accepted Article as a result of editing. Readers should obtain the VoR from the journal website shown below when it is published to ensure accuracy of information. The authors are responsible for the content of this Accepted Article.

To be cited as: *Chem. Eur. J.* 10.1002/chem.202003743

Link to VoR: <https://doi.org/10.1002/chem.202003743>

WILEY-VCH

Photophysical Properties and Heterogeneous Photoredox Catalytic Activities of Ru(bpy)₃@InBTB MOF

In-Hwan Choi,^[a] Sukbin Yoon,^[a] Seong Huh,^{*[a]} Sung-Jin Kim,^[b] and Youngmee Kim^{*[b]}

[a] I.-H. Choi, S. Yoon, Prof. Dr. S. Huh
Department of Chemistry and Protein Research Center for Bio-Industry
Hankuk University of Foreign Studies, Yongin, Korea 17035
E-mail: shuh@hufs.ac.kr

[b] Prof. Dr. S.-J. Kim, Dr. Y. Kim
Institute of Nano-Bio Technology and Department of Chemistry and Nano Science
Ewha Womans University, Seoul, Korea 03760
E-mail: ymeekim@ewha.ac.kr

Supporting information for this article is given via a link at the end of the document.

Abstract: Metal-organic frameworks (MOFs) with negatively charged frameworks are suitable for selectively encapsulating cationic guest ions via a cation-exchange process. Encapsulating photoactive [RuL₃]²⁺ polypyridine complexes into the preorganized mesoscale channels of an MOF is a good method for stabilizing the excited states of the complexes. Three new RuL₃@InBTB MOFs were prepared by encapsulating cationic [Ru(bpy)₃]²⁺ (bpy = 2,2'-bipyridine), [Ru(phen)₃]²⁺ (phen = 1,10-phenanthroline), and [Ru(bpz)₃]²⁺ (bpz = 2,2'-bipyrazine) into the mesopores of a three-dimensional (3D) InBTB MOF (H₃BTB = 1,3,5-benzenetribenzoic acid). The photophysical properties of the resulting materials were investigated by photoluminescence (PL) analysis. The photoredox catalytic activities were also investigated for the aza-Henry reaction, hydrogenation of dimethyl maleate, and decomposition of methyl orange under visible light irradiation at room temperature. RuL₃@InBTB MOFs were found to be very stable and highly recyclable photoredox catalytic systems.

Metal-organic frameworks (MOFs) are multifunctional organic/inorganic hybrid materials with diverse framework structures.^[1] Almost an infinite number of MOFs are possible via simple variation of metal ions and bridging linkers.^[2,3] Solvent-free MOFs can often be employed for a wide range of chemical applications including selective gas sorption,^[4,5] heterogeneous catalysis,^[6,7] and biomedical applications.^[8] Additionally, MOFs with well-defined large open channels can be ideal host materials for the encapsulation of various functional guest molecules or ions.^[9] Catalytically active metal-based nanoparticles (NPs), metal complexes, and organometallic compounds can be captured and stabilized in MOF channels.^[10-12] Especially, MOFs with negatively charged frameworks are suitable for selectively encapsulating cationic guest ions via a simple cation-exchange process with counteranions present in the MOF channels.^[13-16] For example, the InBTB framework with In³⁺ ions and BTB³⁻ linkers formulated as [Et₂NH₂]₃[In₃(BTB)₄·10DEF·14H₂O] (H₃BTB = 1,3,5-benzenetribenzoic acid; DEF = *N,N*-diethylformamide) contains both a negatively charged 3D framework and large mesoscale channels, with a 2-fold interpenetrated network structure containing 71.0% void volume of cation- and solvent-free InBTB (Figure S1).^[13] A very large photoactive Reichardt's dye (RD) was successfully encapsulated into the mesopores of a 3D InBTB MOF. The captured RD cations showed unusual absorption properties due to a confinement effect compared to

free RD in the solid state. In the case of rhodamine 6G (Rh6G) encapsulated InBTB, Rh6G@InBTB exhibited quite distinct fluorescence properties compared to free Rh6G crystals in the solid state.^[14] Thus, this simple encapsulation method can be a good way of capturing guest ions, and guiding the molecular ordering of guests and systematically altering or enhancing their optical properties.

Meanwhile, there is active development of photoredox catalytic systems for various organic transformations.^[17,18] For instance, several [RuL₃]²⁺ polypyridine complexes were successfully employed as visible light-driven photoredox catalysts for a wide range of reactions, such as reductive dehalogenation, radical cyclization, aza-Henry reaction, oxidative biaryl coupling, and so on. Despite their cost-effectiveness, the limitation of [RuL₃]²⁺ polypyridine complex-based photoredox catalysis is the relatively short-lived photoexcited state compared to the cyclometalated Ir(III) complex-based systems.^[17] Furthermore, only a limited number of catalyst immobilization trials using MOFs have been reported

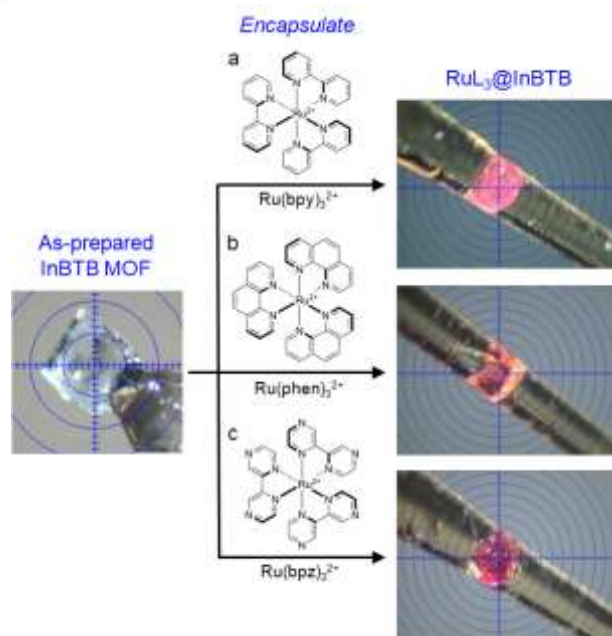


Figure 1. Photo images of colorless as-prepared InBTB and color-changed RuL₃@InBTB MOFs. The chemical structures of [Ru(bpy)₃]²⁺ (a), [Ru(phen)₃]²⁺ (b), and [Ru(bpz)₃]²⁺ (c) are shown together.

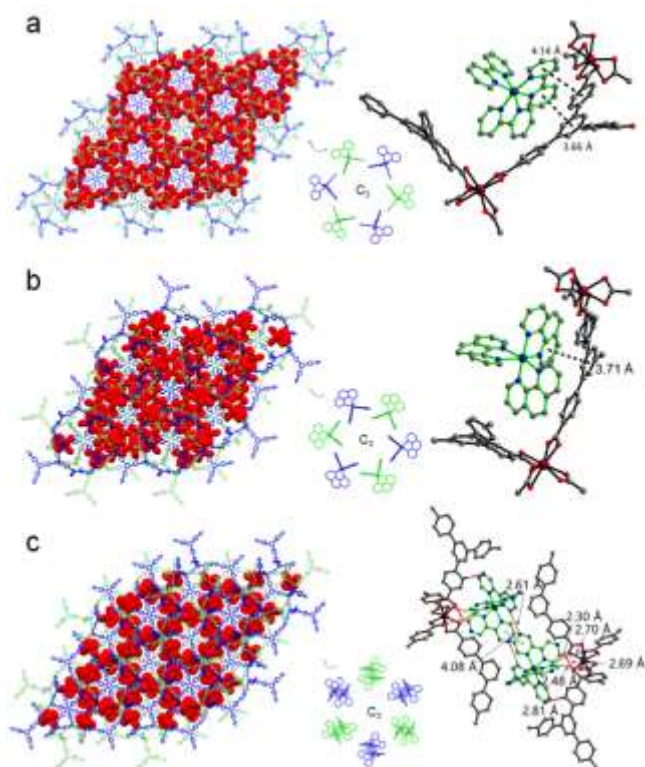


Figure 2. Crystal structures of $\text{Ru}(\text{bpy})_3@ \text{InBTB}$ (a), $\text{Ru}(\text{phen})_3@ \text{InBTB}$ (b), and $\text{Ru}(\text{bpz})_3@ \text{InBTB}$ (c). 2-fold interpenetrated InBTB frameworks are shown using a green and blue stick model, while $[\text{RuL}_3]^{2+}$ ions are shown using a CPK model. The spatial distributions for the $[\text{RuL}_3]^{2+}$ ions and their interactions with InBTB framework are shown together. Black dashed lines indicate $\pi \cdots \pi$ interactions and red dashed lines indicate hydrogen bonding.

in the literature. Amara et al. immobilized $[\text{Ru}(\text{bpy})_3]^{2+}$ onto the surface of nonporous silica for realizing enhanced photochemical oxidation.^[19] There are previous reports on the heterogeneous visible light-driven photoredox aza-Henry catalytic systems.^[19,20] Lin et al. directly coupled dibrominated $[\text{Ru}(\text{bpy})_3]^{2+}$ and $[\text{Ir}(\text{ppy})_2(\text{bpy})]^+$ (ppy = 2-phenylpyridine) moieties with tetra(*p*-ethynylphenyl)methane to prepare polymeric heterogeneous catalysts.^[19] Xi and Xie et al. prepared active heterogeneous photocatalysts based on the covalent organic frameworks (COFs) composed of tetraphenylethylene(TPE)-based electron donor and triazine-based electron acceptor.^[20] Since most photoredox active polypyridine complex-based catalysts are cations, MOFs with negatively charged frameworks can encapsulate these catalysts through simple cation-exchange on the condition that MOF channels are sufficiently large. Relatively strong electrostatic interactions between the anionic framework and metal complex ions will be beneficial for recycling of catalyst. Very recently, Zhou et al. demonstrated a similar recyclable photoredox catalytic system for the aza-Henry reaction using $\text{Ru}(\text{bpy})_3@ \text{PCN-608-SBDC}$ (H_3SBDC = 2-sulfoterephthalic acid).^[22] However, the $\text{Ru}(\text{bpy})_3@ \text{PCN-608-SBDC}$ catalyst was recycled only three times.

To prepare an efficient heterogenized photoredox catalytic system, we attempted to prepare new $\text{RuL}_3@ \text{InBTB}$ MOFs by encapsulating a series of cationic Ru(II) polypyridine derivatives (Figure 1): $[\text{Ru}(\text{bpy})_3]^{2+}$, $[\text{Ru}(\text{phen})_3]^{2+}$, and $[\text{Ru}(\text{bpz})_3]^{2+}$. Their photophysical properties were also

investigated by PL techniques. We selected this Ru(II) series because it exhibits an excellent metal-to-ligand charge transfer (MLCT) transition under visible light irradiation.^[23] These Ru(II) polypyridine complexes are being currently utilized as efficient photoredox catalytic systems for a wide range of organic transformations.^[17,24] Once the excited state lifetime for the encapsulated redox-active $[\text{RuL}_3]^{2+}$ complexes becomes longer than that for the free $[\text{RuL}_3]^{2+}$ complexes, $\text{RuL}_3@ \text{InBTB}$ MOFs can behave as efficient heterogenized photoredox catalytic systems for recycling.

Each Ru(II) derivative was encapsulated into the mesoscale channels of InBTB through cation-exchange with Et_2NH_2^+ counterions in ethanol or acetonitrile solution (2 mM concentration) for 7 d (see Experimental Procedures in the SI). The color change observed for all three RuL_3 -encapsulating crystals indicates clear encapsulation of $[\text{RuL}_3]^{2+}$ in InBTB, as shown in Figure 1. The color-changed InBTB crystals were investigated by X-ray crystallography. The crystal structures for the three $\text{RuL}_3@ \text{InBTBs}$ are depicted in Figure 2. The mesoscale channels in InBTB are sufficiently large enough to accommodate all three $[\text{RuL}_3]^{2+}$ ions. The dimensions of the free $[\text{RuL}_3]^{2+}$ ions are approximately $9.60 \times 9.56 \times 9.48 \text{ \AA}^3$ for $[\text{Ru}(\text{bpy})_3]^{2+}$, $10.07 \times 9.72 \times 9.67 \text{ \AA}^3$ for $[\text{Ru}(\text{phen})_3]^{2+}$, and $9.65 \times 9.63 \times 9.54 \text{ \AA}^3$ for $[\text{Ru}(\text{bpz})_3]^{2+}$. To study the interaction between the framework and $[\text{RuL}_3]^{2+}$ cation complexes, the crystal structure of each $\text{RuL}_3@ \text{InBTB}$ was analyzed, and the occupancies of all $[\text{RuL}_3]^{2+}$ cation atoms were fixed to obtain the best fit with the largest residual peaks (Table S1). The real occupancies were estimated using adsorption data obtained from UV/Vis spectroscopy. The 3-fold rotation axis exists in the center of the BTB^{3-} ligands alternatively along the *c*-axis in $\text{Ru}(\text{bpy})_3@ \text{InBTB}$ and $\text{Ru}(\text{phen})_3@ \text{InBTB}$, and partially occupied $[\text{Ru}(\text{bpy})_3]^{2+}$ and $[\text{Ru}(\text{phen})_3]^{2+}$ cations were attracted to the framework through $\pi \cdots \pi$ interactions (separation distances of 3.66 Å and 4.14 Å for $\text{Ru}(\text{bpy})_3@ \text{InBTB}$ and 3.71 Å for $\text{Ru}(\text{phen})_3@ \text{InBTB}$) with C_3 rotational symmetry alternatively along the *c*-axis (Figure 2a and 2b). Partially occupied pairs of $[\text{Ru}(\text{bpz})_3]^{2+}$ cations exist in the framework with C_3 rotational symmetry alternatively along the *c*-axis, and there are electrostatic interactions between $[\text{Ru}(\text{bpz})_3]^{2+}$ cations and the anionic framework (Figure 2c). In contrast to the $[\text{Ru}(\text{bpy})_3]^{2+}$ cation, two $[\text{Ru}(\text{bpz})_3]^{2+}$ cations are paired through $\pi \cdots \pi$ interaction (separation distance of 4.08 Å) and nonclassical hydrogen bonding interactions (C-H \cdots N 2.61 Å, 139.3°). The N atoms of the bpz ligand may play an important role in the formation of pairs of cations inside the channels. The unit cell dimensions of $\text{RuL}_3@ \text{InBTB}$ deviated to be longer on the *a*- and *b*-axes and shorter on the *c*-axis compared to the dimensions of as-prepared InBTB (Table S1). The cation- and solvent-free $\text{RuL}_3@ \text{InBTBs}$ possess smaller void volumes than the 71.0% void volume based on PLATON analysis: 53.4% for $\text{Ru}(\text{bpy})_3@ \text{InBTB}$, 53.9% for $\text{Ru}(\text{phen})_3@ \text{InBTB}$, and 58.1% for $\text{Ru}(\text{bpz})_3@ \text{InBTB}$. These results indicate that RuL_3^{2+} cations were encapsulated by 12.9 - 17.6% of the original void volume of InBTB.

The uptake amount for each $[\text{RuL}_3]^{2+}$ ion by InBTB was estimated through periodic measurement of the concentration of $[\text{RuL}_3]^{2+}$ ions remaining in the solution by UV/Vis spectroscopy (Figure 3a). The uptake amount of $[\text{Ru}(\text{bpy})_3]^{2+}$, $[\text{Ru}(\text{phen})_3]^{2+}$, and $[\text{Ru}(\text{bpz})_3]^{2+}$, was found to be 0.33 mmol/10 mg-solids, 0.42 mmol/10 mg-solids, and

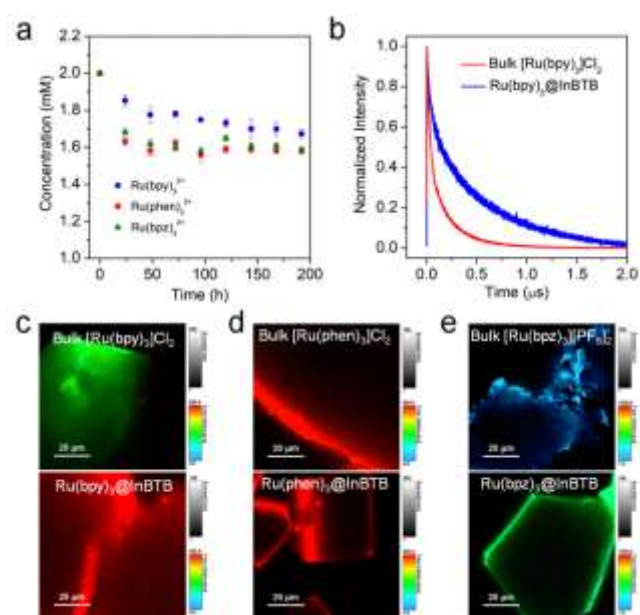


Figure 3. $[RuL_3]^{2+}$ adsorption kinetic curves measured for as-prepared InBTB (a), normalized TRPL decay curves measured for bulk $[Ru(bpy)_3]Cl_2$ and $[Ru(bpy)_3]@InBTB$ upon excitation at 470 nm (b), Fluorescence lifetime imaging (FLIM) images of bulk $[Ru(bpy)_3]Cl_2$ vs. $[Ru(bpy)_3]@InBTB$ (c), bulk $[Ru(phen)_3]Cl_2$ vs. $[Ru(phen)_3]@InBTB$ (d), and bulk $[Ru(bpz)_3][PF_6]_2$ vs. $[Ru(bpz)_3]@InBTB$ (e).

0.42 mmol/10 mg-solids, respectively. Thus, the encapsulation amount for the $[Ru(bpy)_3]^{2+}$ ion is slightly smaller than that for the $[Ru(phen)_3]^{2+}$ and $[Ru(bpz)_3]^{2+}$ ions. A fluorescence confocal laser scanning microscopy (CLSM) investigation of the $RuL_3@InBTB$ crystals indicated uniform distribution of phosphorescent $[RuL_3]^{2+}$ ions over the entire crystal (Figure S2). However, the central part of the crystal indicates less intense emission, and this implies that the penetration of $[RuL_3]^{2+}$ ions into the mesopores was not completely achieved. Pore blocking by initially exchanged $[RuL_3]^{2+}$ ions may prevent complete exchange.

We investigated the PL properties of $[Ru(bpy)_3]@InBTB$ crystals in the solid state. The $[Ru(bpy)_3]^{2+}$ ion in acetonitrile absorbs the visible range of light centered at a wavelength of 452 nm due to an efficient 1MLCT transition.^[23] The excited 1MLCT state quickly relaxes to a lowest-energy 3MLCT state through the intersystem crossing (ISC) process. Thus, an intense 3MLCT emission band centered at 620 nm was observed upon excitation by visible light. The same band was seen at 607 nm in aqueous solution.^[25] Interestingly, the solid-state PL spectrum of $[Ru(bpy)_3]@InBTB$ revealed a strong 3MLCT emission band centered at 598 nm ($\lambda_{ex} = 450$ nm) (Figure S3). Therefore, the encapsulation of the $[Ru(bpy)_3]^{2+}$ ion induced a blueshifted PL emission band. Contrarily, the emission band position for $[Ru(phen)_3]@InBTB$ is very similar to that for the free $[Ru(phen)_3]^{2+}$ ion in aqueous solution, 604 nm vs. 610 nm ($\lambda_{ex} = 422$ nm).^[17] In stark contrast, $[Ru(bpz)_3]@InBTB$ displayed a redshifted emission band at 619 nm ($\lambda_{ex} = 443$ nm), while the free $[Ru(bpz)_3]^{2+}$ ion in acetonitrile showed a band centered at 591 nm.^[25] The origin of this difference can be attributed to the dimeric form of $[Ru(bpz)_3]^{2+}$ ions in $[Ru(bpz)_3]@InBTB$. The unique spatial orientations of $[Ru(bpy)_3]^{2+}$

and $[Ru(bpz)_3]^{2+}$ ions and distinct nanoscale environments in the InBTB channels dramatically altered the PL properties.

The time-resolved photoluminescence (TRPL) decay curves for the solid samples were also measured to compare the excited state lifetimes of bulk $[Ru(bpy)_3]^{2+}$ and $[Ru(bpy)_3]@InBTB$, as depicted in Figure 3b. Interestingly, the fitted curves indicate that the amplitude average lifetime of $[Ru(bpy)_3]^{2+}$ captured in $[Ru(bpy)_3]@InBTB$ ($\tau = 420 \pm 2.8$ ns) is much longer than the control bulk sample ($\tau = 114 \pm 0.11$ ns). This means that the captured $[Ru(bpy)_3]^{2+}$ ions maintain a triplet excited state (3MLCT) more effectively than the bulk sample through retarding nonradiative decay.^[26] $[Ru(bpz)_3]@InBTB$ showed similar behavior (Figure S4). Contrarily, $[Ru(phen)_3]@InBTB$ is an exceptional case. $[Ru(phen)_3]@InBTB$ showed an unusually shorter decay lifetime than that for bulk $[Ru(phen)_3]Cl_2$. The fluorescence lifetime imaging (FLIM) images shown in Figure 3c-3e also clearly indicate that the captured $[Ru(bpy)_3]^{2+}$ and $[Ru(bpz)_3]^{2+}$ ions exhibit longer luminescence lifetimes than the bulk samples. These results suggest that encapsulation of Ru(II) polypyridine complexes into MOF channels is a good method to enhance their PL lifetimes.^[26,27] Furthermore, $[Ru(bpy)_3]@InBTB$ and $[Ru(bpz)_3]@InBTB$ with long-lived excited states can be employed as efficient photoredox catalytic systems for organic transformations and other optical applications. The redox potentials of $[Ru(bpy)_3]@InBTB$ were estimated from the cyclic voltammogram as shown in Table S2. The values are comparable to those of the free $[Ru(bpy)_3]^{2+}$ ion.^[17]

Encouraged by these promising results, the catalytic activities of $RuL_3@InBTB$ were investigated for the photoredox aza-Henry reaction of 2-phenyl-1,2,3,4-tetrahydroisoquinoline (THIQ) with nitromethane under visible light irradiation using a commercial fluorescent lamp (20 W), as shown in Figure 4a and Figure S5. In the aza-Henry reaction, the tertiary amine substrate is oxidized to an iminium ion via an aminium radical cation in the aerobic condition, which further reacts with nitromethane to give the desired coupled product.^[17,28] Thus, photoactivated $[RuL_3]^{2+}$ species can act as an oxidant for the THIQ substrate in the first step of the previously proposed reaction pathway (Figure S6).^[17] In the screening experiments, $[Ru(bpy)_3]@InBTB$ displayed a slightly higher product selectivity ($S = 71\%$; the selectivity S is defined by the ratio of the desired C-C coupled product to the conversion of the substrate) despite its lower conversion than $[Ru(phen)_3]@InBTB$ ($S = 67\%$) and $[Ru(bpz)_3]@InBTB$ ($S = 68\%$) (Figure S5). The product yield for the desired product increases in the order of $[Ru(bpy)_3]@InBTB$ (46%) < $[Ru(phen)_3]@InBTB$ (56%) < $[Ru(bpz)_3]@InBTB$ (63%). A control experiment under visible light without catalysts showed that the reaction can also give the product with a much lower selectivity ($S = 53\%$). Another control experiment using as-prepared InBTB alone under visible light showed a very similar result with a low selectivity ($S = 50\%$). Thus, as-prepared InBTB cannot itself catalyze the reaction. We chose $[Ru(bpy)_3]@InBTB$ catalyst for recycling experiments because it showed the highest product selectivity. $[Ru(bpy)_3]@InBTB$ can be recycled up to nine times without significant loss of activity and product selectivity (Figure 4b). This capacity illustrates that $[Ru(bpy)_3]@InBTB$ is a stable recyclable photoredox catalytic system for the aza-Henry reaction. Notably, both the conversion and product yield gradually increased upon recycling. We did not expect these gradual increases of activities because the

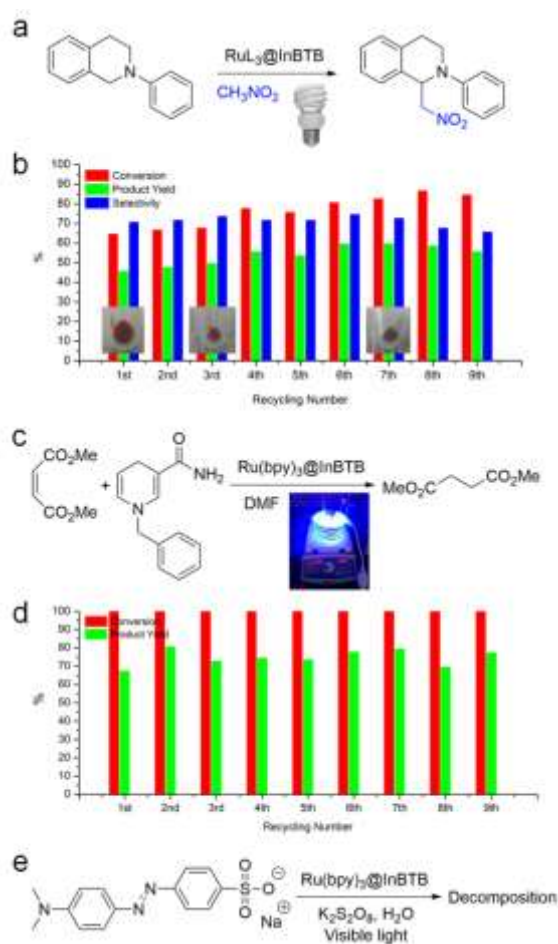


Figure 4. (a) Catalytic aza-Henry reaction of THIQ. (b) Recycling results for the aza-Henry reaction by $\text{Ru}(\text{bpy})_3@ \text{InBTB}$. Photographic images of the retrieved catalyst after the 1st, 3rd, and 7th runs are shown together. (c) Catalytic hydrogenation of dimethyl maleate in the presence of BNAH. (d) Recycling results obtained for the corresponding hydrogenation. (e) Photodecomposition of methyl orange by $\text{Ru}(\text{bpy})_3@ \text{InBTB}$ in the presence of $\text{K}_2\text{S}_2\text{O}_8$.

recovery of the used catalyst for recycling could not be perfect. Generally, the activity may gradually decrease due to small loss of catalyst. We speculate that there were iminium ions derived from the substrate in the reaction mixture for aza-Henry reaction, and these ions could replace some of the remaining diethylammonium ions in $\text{Ru}(\text{bpy})_3@ \text{InBTB}$. This process could enhance the activity upon recycling. The doubly charged $[\text{Ru}(\text{bpy})_3]^{2+}$ ions should be more resistant to this cation exchange.

From a mechanistic point of view, the cationic iminium intermediate can be captured in the channels of as-prepared InBTB during the reaction, thus the FT-IR spectra for as-prepared InBTB and the retrieved InBTB after the control experiment were collected to probe distinct features (Figure S7). The InBTB used showed a new signal attributable to the iminium moiety ($\text{C}=\text{N}^+$) derived from THIQ at 1698 cm^{-1} , while this signal was absent in the spectrum measured for the as-prepared InBTB.^[29] Concomitantly, the characteristic $\text{C}=\text{O}$ signal due to DEF solvates at 1657 cm^{-1} in the as-prepared InBTB completely disappeared. Additionally, the initially

colorless InBTB crystals showed a color change to a reddish color after the control reaction, indicating the possible encapsulation of the iminium intermediate (Figure S8). Although the X-ray analysis of the used InBTB containing iminium ions was not successful, these results clearly confirm the formation of an iminium species during the reaction.

To further demonstrate the versatility of the $\text{Ru}(\text{bpy})_3@ \text{InBTB}$ catalyst, its activity for the hydrogenation of electron-deficient dimethyl maleate to dimethyl succinate in the presence of 1-benzyl-1,4-dihydronicotinamide (BNAH) as a hydrogen source was tested by using a blue LED (7 W) as a light source at room temperature (Figure 4c). $[\text{Ru}(\text{bpy})_3]^{2+}$ was reported to effectively catalyze this hydrogenation.^[30] This hydrogenation is a good model reaction for a photoredox hydrogenation catalyst. $\text{Ru}(\text{bpy})_3@ \text{InBTB}$ serves as an oxidant in the first reductive quenching cycle of BNAH during the proposed reaction pathway (Figure S9).^[17,30] The photoexcited $[\text{Ru}(\text{bpy})_3]^{2+}$ accepts an electron from BNAH to generate a BNAH cation radical, $\text{BNAH}^{\cdot+}$, in the proposed catalytic cycle. In deoxygenated DMF, $\text{Ru}(\text{bpy})_3@ \text{InBTB}$ successfully catalyzed the reaction up to nine times without loss of activity (Figure 4d). While the reaction conversions are $\sim 100\%$ for each reaction, the product yields are in the range 68–81%. The initial product yield (68%) is slightly different from that of the ninth reaction (78%). Unwanted byproducts were usually observed in this two-electron reduction process, and they are the coupled product of a BNA^{\cdot} radical with dimethyl maleate or the dimeric form of BNA^{\cdot} radicals.^[30] These results clearly confirm that the heterogeneous $\text{Ru}(\text{bpy})_3@ \text{InBTB}$ is a good heterogeneous photoredox hydrogenation catalyst with high recyclability.

We further explored the visible light-driven photocatalytic decomposition of methyl orange (MO) in the presence of potassium persulfate, $\text{K}_2\text{S}_2\text{O}_8$, by using $\text{Ru}(\text{bpy})_3@ \text{InBTB}$ as a photocatalyst and a solar simulator (150 W) as a visible light source (Figure 4e). Since the reaction solvent is deionized water, this reaction also presents a good method to investigate the stability of the $\text{Ru}(\text{bpy})_3@ \text{InBTB}$ system. The photoexcited $[\text{Ru}(\text{bpy})_3]^{2+}$ ions tend to cleave the $\text{S}_2\text{O}_8^{2-}$ ion into two $\text{SO}_4^{\cdot-}$ radical anions, which further react with water to generate HO^{\cdot} . Both $\text{SO}_4^{\cdot-}$ and HO^{\cdot} radicals are likely to be responsible for the decomposition of MO (Figure S10).^[31] The $\text{Ru}(\text{bpy})_3@ \text{InBTB}$ photoredox catalyst efficiently generated reactive radicals and successfully decomposed MO. Interestingly, the $\text{Ru}(\text{bpy})_3@ \text{InBTB}$ catalyst could be recycled at least five times (Figure S11). The catalytic activities for all five runs were maintained at similar levels.

The PXRD patterns of each recovered catalyst after recycling experiments indicated relatively weak and broad diffraction signals as shown in Figure S12. The diffraction signals of $\text{Ru}(\text{bpy})_3@ \text{InBTB}$ before catalytic reactions also showed very broad signals indicating partial loss of crystallinity. Nonetheless, the microscopic image of $\text{Ru}(\text{bpy})_3@ \text{InBTB}$ crystals before catalytic reaction did not show any significant change of crystal shapes as depicted Figure S13. More importantly, the $\text{Ru}(\text{bpy})_3@ \text{InBTB}$ crystals after nine times of hydrogenation of dimethyl maleate performed in DMF solvent exhibited much enhanced diffraction peaks. These observations suggest that the residual DEF and water solvate molecules in InBTB might be exchanged with EtOH or nitromethane used for $\text{Ru}(\text{II})$ complex encapsulation and catalytic reactions to show broad and weak diffraction signals. Therefore, despite the

partial loss of crystallinity due to exchange of solvate molecules, the metal-ligand connectivities and 3D framework were well preserved.

In summary, we successfully prepared new optical materials containing luminescent Ru(II) polypyridine complexes using a mesoporous InBTB MOF through a simple cation-exchange process. The crystal structures for RuL₃@InBTB were determined to locate the spatial positions of the [RuL₃]²⁺ ions. Ru(bpy)₃@InBTB and Ru(bpz)₃@InBTB exhibited extended PL emission lifetimes compared to the bulk crystalline samples. These features render such complexes to be good heterogeneous photoredox catalytic systems with high recyclability. We envision that many other photoredox catalysts can be similarly immobilized into MOF channels in a very simple manner without losing their catalytic activities.

Acknowledgements

This work was supported by the Basic Science Research Program of the National Research Foundation of Korea (NRF), which was funded by the Ministry of Education, Science and Technology (2018R1D1A1B07043017 and 2018R1D1A1B07045327).

Conflict of interest

The authors declare no conflict of interest.

Keywords: metal-organic framework • ruthenium complex • photoredox catalysis • aza-Henry reaction • hydrogenation

- [1] H. Furukawa, K. E. Cordova, M. O'Keeffe, O. M. Yaghi, *Science* **2013**, *341*, 1230444.
- [2] O. M. Yaghi, M. O'Keeffe, N. W. Ockwig, H. K. Chae, M. Eddaoudi, J. Kim, *Nature* **2003**, *423*, 705-714.
- [3] S. Kitagawa, R. Kitaura, S.-i. Noro, *Angew. Chem. Int. Ed.* **2004**, *43*, 2334-2375.
- [4] K. Sumida, D. L. Rogow, J. A. Mason, T. M. McDonald, E. D. Bloch, Z. R. Herm, T.-H. Bae, J. R. Long, *Chem. Rev.* **2012**, *112*, 724-781.
- [5] H.-G. Hao, Y.-F. Zhao, D.-M. Chen, J.-M. Yu, K. Tan, S. Ma, Y. Chabal, Z.-M. Zhang, J.-M. Dou, Z.-H. Xiao, G. Day, H.-C. Zhou, T.-B. Lu, *Angew. Chem. Int. Ed.* **2018**, *57*, 16067-16071.
- [6] G. Kumar, S. K. Das, *Inorg. Chem. Front.* **2017**, *4*, 202-233.
- [7] A. H. Chughtai, N. Ahmad, H. A. Younus, A. Laypkov, F. Verpoort, *Chem. Soc. Rev.* **2015**, *44*, 6804-6849.
- [8] L. Wang, M. Zheng, Z. Xie, *J. Mater. Chem. B* **2018**, *6*, 707-717.
- [9] Y. Cui, B. Li, H. He, W. Zhou, B. Chen, G. Qian, *Acc. Chem. Res.* **2016**, *49*, 483-493.
- [10] G. Li, S. Zhao, Y. Zhang, Z. Tang, *Adv. Mater.* **2018**, *30*, 1800702.
- [11] C. R. Kim, T. Uemura, S. Kitagawa, *Chem. Soc. Rev.* **2016**, *45*, 3828-3845.
- [12] L. Chen, R. Luque, Y. Li, *Dalton Trans.* **2018**, *47*, 3663-3668.
- [13] E.-Y. Cho, J.-M. Gu, I.-H. Choi, W.-S. Kim, Y.-K. Hwang, S. Huh, S.-J. Kim, Y. Kim, *Cryst. Growth Des.* **2014**, *14*, 5026-5033.
- [14] I.-H. Choi, S. B. Yoon, S. Huh, S.-J. Kim, Y. Kim, *Sci. Rep.* **2018**, *8*, 9838.
- [15] A. Grigoropoulos, G. F. S. Whitehead, N. Perret, A. P. Katsoulidis, F. M. Chadwick, R. P. Davies, A. Haynes, L. Brammer, A. S. Weller, J. Xiao, M. J. Rosseinsky, *Chem. Sci.* **2016**, *7*, 2037-2050.
- [16] J. Yu, Y. Cui, C. Wu, Y. Yang, Z. Wang, M. O'Keeffe, B. Chen, G. Qian, *Angew. Chem. Int. Ed.* **2012**, *51*, 10542-10545.
- [17] C. K. Prier, D. A. Rankic, D. W. C. MacMillan, *Chem. Rev.* **2013**, *113*, 5322-5363.
- [18] D. M. Schultz, T. P. Yoon, *Science* **2014**, *343*, 1239176.
- [19] C. Wang, Z. Xie, K. E. deKrafft, W. Lin, *ACS Appl. Mater. Interfaces* **2012**, *4*, 2288-2294.
- [20] Q. Liao, W. Xu, X. Huang, C. Ke, Q. Zhang, K. Xi, J. Xie, *Sci. China Chem.* **2020**, *63*, 707-714.
- [21] B. Tambosco, K. Segura, C. Seyrig, D. Cabrera, M. Port, C. Ferroud, Z. Amara, *ACS Catal.* **2018**, *8*, 4383-4389.
- [22] J. Pang, S. Yuan, J.-S. Qin, C. T. Lollar, N. Huang, J. Li, Q. Wang, M. Wu, D. Yuan, M. Hong, H.-C. Zhou, *J. Am. Chem. Soc.* **2019**, *141*, 3129-3136.
- [23] D. M. Arias-Rotondo, J. K. McCusker, *Chem. Soc. Rev.* **2016**, *45*, 5803-5820.
- [24] J. M. R. Narayanam, C. R. J. Stephenson, *Chem. Soc. Rev.* **2011**, *40*, 102-113.
- [25] M.-A. Haga, E. S. Dodsworth, G. Eryavec, P. Seymour, A. B. P. Lever, *Inorg. Chem.* **1985**, *24*, 1901-1906.
- [26] L. Wang, W. Yang, Y. Li, Z. Xie, W. Zhu, Z.-M. Sun, *Chem. Commun.* **2014**, *50*, 11653-11656.
- [27] H. Xu, J. Gao, J. Wang, X. Qian, R. Song, Y. Cui, Y. Yang, G. Qian, *J. Solid State Chem.* **2015**, *226*, 295-298.
- [28] H. Bartling, A. Eisenhofer, B. König, R. M. Gschwind, *J. Am. Chem. Soc.* **2016**, *138*, 11860-11871.
- [29] G. R. Clark, G. L. Shaw, P. W. J. Surman, M. J. Taylor, *J. Chem. Soc. Faraday Trans.* **1994**, *90*, 3139-3144.
- [30] C. Pac, M. Ihama, M. Yasuda, Y. Miyauchi, H. Sakurai, *J. Am. Chem. Soc.* **1981**, *103*, 6495-6497.
- [31] L. W. Matzek, K. E. Carter, *Chemosphere* **2016**, *151*, 178-188.

Entry for the Table of Contents



Photoactive cationic Ru(II) polypyridine complexes can be effectively encapsulated into mesoscale channels of an InBTB metal-organic framework to afford heterogenized photoredox catalytic systems, $\text{RuL}_3@ \text{InBTB}$. $\text{Ru}(\text{bpy})_3@ \text{InBTB}$ showed a longer excited state lifetime compared to the free ion and displayed highly recyclable catalytic activities for the aza-Henry reaction, hydrogenation of methyl maleate, and decomposition of methyl orange under visible light irradiation.

Institute and/or researcher Twitter usernames: ((optional))